IJAME

Int. J. of Applied Mechanics and Engineering, 2023, vol.28, No.2, pp.49-63
DOI: 10.59441/ijame/168331

LUBRICATION OF ASYMMETRIC ROLLERS CONSIDERING VISCOSITY AS FUNCTION OF MEAN TEMPERATURE

Swetha Lanka
Research Scholar, Department of Engineering Mathematics, Koneru Lakshmaiah Education Foundation Guntur-522502, INDIA
Department of Mathematics, Sir C R Reddy College of Engineering, Eluru-534007, A.P., INDIA

Venkata Subrahmanyam Sajja*
Department of Engineering Mathematics, Koneru Lakshmaiah Education Foundation Guntur-522502, INDIA
E-mail: subrahmanyam@kluniversity.in

Dhaneshwar Prasad
Department of Mathematics, Kanchi Mamunivar Government Institute for Post Graduate Studies and Research, Puducherry-605008, INDIA

A theoretical analysis of an asymmetric roller bearing system with cavitation that is hydro-dynamically lightly loaded and lubricated by a thin, incompressible fluid is presented. The lubricant adheres to the non-Newtonian Bingham plastic fluid concept, in which the viscosity of the fluid should change depending on the mean film temperature. The continuity and momentum equations, which regulate fluid flow, are first solved analytically and then numerically using MATLAB. Through graphs and tables, some key bearing features are addressed and further explained. This leads to the conclusion that there is a discernible difference between Newtonian and non-Newtonian fluids in terms of pressure, temperature, load, and traction. The findings are good in line with the body of literature.

Keywords: non-Newtonian, Bingham plastic, hydrodynamic lubrication, incompressible, viscosity.

1. Introduction

Many technical applications depend on the fluid film lubrication technique, which is widely used in machine devices, motors, super gadgets, cams and skeletal joints [1].

On surfaces that are subject to fluid scouring, hydrodynamic lubrication is a technique used to reduce wear and friction. Adding the right liquid with the intention that it penetrates the contact area between the scouring surfaces and creates a thin layer is the typical purpose of hydrodynamic lubrication. This coating effectively lowers friction and wear by keeping the surfaces from coming into touch. Extremely high loads, peak speeds, and extreme slip situations are ongoing demands placed on bearings. For example, the viscosity of oil varies continuously with temperature and pressure in the high pressure area [2].

Using an incompressible power-law fluid, Prasad *et al.* [2] published a study on the thermo-hydrodynamic lubrication of line contact. There is a significant difference between Newtonian and non-Newtonian fluids in terms of temperature, pressure, load, and traction, according to the pressure and heat equations, which depend on the consistency, rolling ratio, and power-law parameter. In order to investigate the thermo-hydrodynamic effect for substantially loaded journal bearings, Prasad *et al.* [1] used the power-law model. The load ratio drops with a rise in the power-law index "*n*", which is based on the assumption that the lubricant's consistency

* To whom correspondence should be addressed

changes with both pressure and also mean temperature. Using incompressible, power-law lubricants, including Newtonian, in isothermal and adiabatic conditions, Sajja and Prasad [3] investigated the theoretical characterization of HDL of anti-symmetric surfaces. The load with the flow index "*n*" and pressure both significantly increase for a constant value of the rolling ratio parameter.

The properties of a non-Newtonian Bingham plastic fluid flow have long been used to describe the behaviour of fluids in general. Additionally, they have been used to show how melts and slurries behave in moulds and during designed handling [4, 5]. The basic slider bearing and journal bearing in one dimension were the subject of investigation, and a it was concluded that any surface might have had rigid "cores" added to it. In addition, Christopher Dorier and John Tichy introduced a model of the behaviour of fluids that are similar to Bingham's, which exhibit a yield stress [4]. Revathi *et al.* [6] recently investigated non-Newtonian lubrication of asymmetric rollers for a highly stacked rigid system using an incompressible Bingham plastic fluid in rolling/sliding line contact while modifying the fluid viscosity with hydrodynamic pressure. The findings, particularly the pressure, load, and traction forces, are well in line with the body of currently available literature. Distributions of lubricant velocity are shown. Additionally, Revathi *et al.* [7] investigated a topic pertaining to the lubricating properties of anti-symmetric rollers using a non-Newtonian incompressible Bingham plastic fluid. For both Newtonian and non-Newtonian fluids, the temperatures, pressures, loads, and traction forces, in particular, are in good agreement with prior findings.

The goal of this study, in light of the aforementioned discussion, is to examine the thermal effects of an incompressible Bingham plastic fluid used to lubricate asymmetric rollers in a lightly loaded rolling/sliding inelastic system under the behaviour of line contact. The viscosity of the lubricant follows Roelands model and changes with pressure and temperature. Rolling ratios are used to assess how pressure, load, and traction are affected as surfaces slide and roll. It is presumed that the viscosity changes with mean temperature.

2. Theoretical model

A lightly loaded rigid system with asymmetric roller bearings using non-Newtonian incompressible lubricant is considered in this work to account for the Bingham plastic fluid. Both surfaces in this study have the same radius and are moving at different velocities. The fact that the lower surface is moving faster than the upper surface is also obvious. The physical diagram of the flow pattern is presented in Fig. (1).

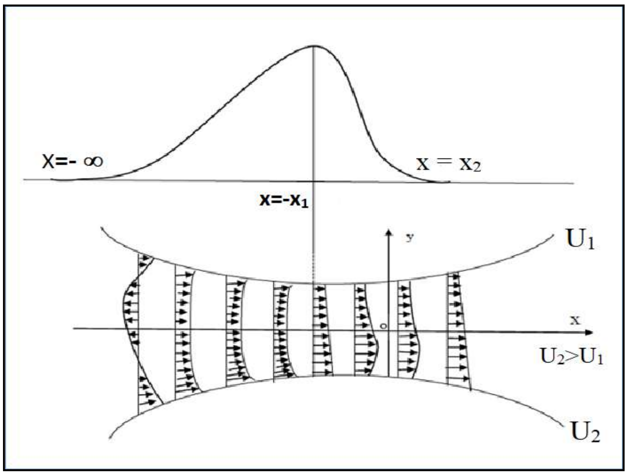

Fig.1. Lubrication of asymmetric rollers

2.1. Theoretical model

Under common presumptions [8], the following governing equations, which regulate the incompressible fluids flow, are taken into account:

$$\frac{\partial u}{\partial x}+\frac{\partial v}{\partial y}=0\,, \tag{2.1}$$

$$\frac{dp}{dx}=\frac{\partial \tau}{\partial y} \tag{2.2}$$

where, respectively, “p” denotes the hydrodynamic pressure and “τ” the lubricant shear stress. For a Bingham plastic fluid, the fundamental equation is provided by [9]:

$$\tau=\pm\,\tau_0+\mu\frac{\partial u}{\partial y} \tag{2.3}$$

where μ is the lubricant viscosity taken by [10]:

$$\mu=\mu_0 e^{-\beta\,(T_m-T_0)} \tag{2.4}$$

and equation to be used to determine the film's thickness is

$$h=h_0+\frac{x^2}{2R} \tag{2.5}$$

R represents the radius of the ‘equivalent cylinder’.

2.2. Boundary conditions

For this problem, the upper and lower surfaces boundary conditions are assumed to be

$$u=U_1 \quad \text{at} \quad y=h, \tag{2.6}$$

$$u=U_2 \quad \text{at} \quad y=-h, \tag{2.7}$$

$$p=0 \quad \text{at} \quad x=-\infty, \tag{2.8}$$

$$p=0 \quad \text{and} \quad \frac{dp}{dx}=0 \quad \text{at} \quad x=x_2 \tag{2.9}$$

where U_1 and U_2 are speeds of the rollers.

Equation (2.2) is integrated by making use of the aforementioned “boundary conditions” to produce the fluid velocity expression shown below.

$$u=\frac{3(y^2-h^2)(U_1+U_2)(h-h_1)}{4h^3}+\frac{y}{2h}(U_1-U_2)+\frac{1}{2}(U_1+U_2)\,. \tag{2.10}$$

The above velocity is integrated in the area between the surfaces to get the “volume flux, Q” for the “fluid flow”, which is provided below

$$Q=\int_{-h}^{h} u dy = h\left(U_1+U_2\right)-\frac{2h^3}{3\mu}\frac{dp}{dx} \tag{2.11}$$

and the 'volume flux' at the pressure's peak is:

$$Q\left(-x_1\right)=\left(U_1+U_2\right)h_1 \tag{2.12}$$

where the "film thickness" h_1 at $x=-x_1$ is considered to be $h_1=1+x_1^2$.

2.3. Reynolds equation

The above boundary conditions can be used to solve Eq.(2.2) and obtain the pressure Reynolds equation as presented below.

$$\frac{dp}{dx}=\frac{3\mu}{2h^3}\left[\left(U_1+U_2\right)\left(h-h_1\right)\right]. \tag{2.13}$$

2.4. Scheme for non-dimensionalization

The following non-dimensional technique is utilised in this article.

$$\bar{x}=\frac{x}{R},\quad \bar{h}=1+\bar{x}^2,\quad \bar{\mu}=\overline{\mu_0}e^{-\left(\overline{T_m}-\overline{T_0}\right)},\quad \overline{\tau_0}=\frac{R\tau_0}{h_0},$$

$$\overline{\mu_0}=\frac{2RU}{h_0^2}\mu_0,\quad \bar{U}=U_2/U_1,\quad \overline{T_m}=\beta T_m.$$

Using the aforementioned dimensionless technique, the velocity and pressure equation are represented in a dimensionless form.

$$\bar{u}=\frac{3\left(1+\bar{U}\right)\left(\bar{h}-\overline{h_1}\right)\left(\bar{y}^2-\bar{h}^2\right)}{4\bar{h}^3}+\frac{\bar{y}}{2\bar{h}}\left(1-\bar{U}\right)+\frac{1}{2}\left(1+\bar{U}\right), \tag{2.14}$$

$$\frac{d\bar{p}}{d\bar{x}}=\frac{3\bar{\mu}\left(1+\bar{U}\right)\left(\bar{h}-\overline{h_1}\right)}{4\bar{h}^3}. \tag{2.15}$$

2.5. Heat equation

Assume the line contact lubrication problem with the following heat equation [3]:

$$\rho c_p\left(u_m\frac{dT_m}{dx}\right)=k\frac{\partial^2 T}{\partial y^2}+\tau\frac{\partial u}{\partial y}. \tag{2.16}$$

The Eq.(2.3) is used to derive the shear stress for the Bingham plastic fluid.

The following describe the heat equation's boundary conditions.

$$T=T_U \text{ at } y=h \text{ and } T=T_L \text{ at } y=-h. \tag{2.17}$$

The temperature of the lubricant is shown below as a result of integration of Eq.(2.16):

$$\begin{aligned}
T=&\left(\frac{\rho C_p}{2k}\right)\left(u_m\frac{dT}{dx}\right)\left(y^2-h^2\right)+\left(\frac{T_U-T_L}{2h}\right)y+\left(\frac{T_U+T_L}{2}\right)-\\
&+\left(\frac{\tau_0}{k}\right)\left[\left(\frac{(U_1-U_2)}{4h}\right)\left(y^2-h^2\right)+\left(\frac{(U_1+U_2)(h-h_1)}{4h^3}\right)\left(y^3-h^2y\right)\right]+\\
&-\left(\frac{\mu}{k}\right)\left[\left(\frac{(U_1-U_2)^2}{8h^2}\right)\left(y^2-h^2\right)+\left(\frac{3(U_1+U_2)^2(h-h_1)^2}{16h^6}\right)\left(y^4-h^4\right)+\right.\\
&\left.+\left(\frac{(U_1+U_2)(U_1-U_2)(h-h_1)}{4h^4}\right)\left(y^3-h^2y\right)\right].
\end{aligned}\tag{2.18}$$

Thus, the explicit relationship between x and y and the temperature "T" is known analytically. The mean film temperature is now provided by $T_m=\int_{-h}^{h}Tdy$ and obtained as:

$$\begin{aligned}
T_m=&\left(\frac{T_U+T_L}{2}\right)-\left(\frac{\rho C_p h^2}{3k}\right)\left(u_m\frac{dT_m}{dx}\right)+\left(\frac{\tau_0}{k}\right)\left(\frac{h(U_1-U_2)}{6}\right)+\\
&+\left(\frac{\mu}{k}\right)\left[\left(\frac{3(U_1+U_2)^2(h-h_1)^2}{20h^2}\right)+\left(\frac{(U_1-U_2)^2}{12}\right)\right].
\end{aligned}\tag{2.19}$$

Now, the "temperature and mean temperature" in a dimensionless form are produced as shown below:

$$\begin{aligned}
\overline{T}=&\left(\frac{3}{2}\overline{P_e}\frac{d\overline{T_m}}{d\overline{x}}\right)\left(\overline{y}^2-\overline{h}^2\right)+\left(\frac{\overline{T_U}-\overline{T_L}}{2\overline{h}}\right)\overline{y}+\left(\frac{\overline{T_U}+\overline{T_L}}{2}\right)-\\
&+\overline{\lambda}\left[\left(\frac{(1-\overline{U})}{4\overline{h}}\right)\left(\overline{y}^2-\overline{h}^2\right)+\left(\frac{(1+\overline{U})(\overline{h}-\overline{h_1})}{4\overline{h}^3}\right)\left(\overline{y}^3-\overline{h}^2\overline{y}\right)\right]-\\
&+\overline{\gamma}\overline{\mu}\left[\left(\frac{(1-\overline{U})^2}{8\overline{h}^2}\right)\left(\overline{y}^2-\overline{h}^2\right)+\left(\frac{3(1+\overline{U})^2(\overline{h}-\overline{h_1})^2}{16\overline{h}^6}\right)\left(\overline{y}^4-\overline{h}^4\right)+\right.\\
&\left.++\left(\frac{(1+\overline{U})(1-\overline{U})(\overline{h}-\overline{h_1})}{4\overline{h}^4}\right)\left(\overline{y}^3-\overline{h}^2\overline{y}\right)\right],
\end{aligned}\tag{2.20}$$

$$\overline{T_m} = \left(\frac{\overline{T_U} + \overline{T_L}}{2}\right) - \left(\overline{P_e}\,\overline{h}^2 \frac{d\overline{T_m}}{d\overline{x}}\right) + \overline{\lambda}\left(\frac{\overline{h}\left(1-\overline{U}\right)}{6}\right) + \\ + \overline{\gamma}\,\overline{\mu}\left[\left(\frac{\left(1-\overline{U}\right)^2}{12}\right) + \left(\frac{3\left(1+\overline{U}\right)^2\left(\overline{h}-\overline{h_1}\right)^2}{20\overline{h}^2}\right)\right], \tag{2.21}$$

$$\frac{d\overline{T_m}}{d\overline{x}} = \frac{1}{\overline{P_e}\,\overline{h}^2}\left\{\left(\frac{\overline{T_U} + \overline{T_L}}{2}\right) - \overline{T_m} + \overline{\lambda}\left(\frac{\overline{h}\left(1-\overline{U}\right)}{6}\right) + \\ + \overline{\gamma}\,\overline{\mu}\left[\left(\frac{\left(1-\overline{U}\right)^2}{12}\right) + \left(\frac{3\left(1+\overline{U}\right)^2\left(\overline{h}-\overline{h_1}\right)^2}{20\overline{h}^2}\right)\right]\right\} \tag{2.22}$$

where $\overline{\lambda} = \left(\frac{\tau_0 \beta U_1 h_0}{k}\right)$, $\overline{P_e} = \left(\frac{\rho C_p u_m h_0^2}{3kR}\right)$, $\overline{\gamma} = \left(\frac{\beta U_1 h_0^2}{2kR}\right)$.

2.6. Load and traction [3]

One crucial factor is load capacity since it provides a precise assessment of the bearings efficiency. Integrate the pressure along the x-axis to calculate the normal load carrying capability

$$W_y = \int_{-\infty}^{x_2} p\,dx\,. \tag{2.23}$$

The normal load $\overline{W_y}$ in a dimensionless form is given by

$$\overline{W}_y = \int_{-\infty}^{\overline{x}_2} \overline{p}\,d\overline{x} = -\int_{-\infty}^{\overline{x}_2} \overline{x}\,\frac{d\overline{p}}{d\overline{x}}\,d\overline{x}\,. \tag{2.24}$$

The traction forces "T_F" at both the surfaces can also be calculated by integrating the "shear stress" along the entire length.

$$T_{Fh-} = -\int_{-\infty}^{x_2} \tau_{y=-h}\,dx \quad \text{and} \quad T_{Fh+} = -\int_{-\infty}^{x_2} \tau_{y=h}\,dx\,. \tag{2.25}$$

The tractions in a non-dimensional form are:

$$\overline{T}_{Fh-} = -\int_{-\infty}^{\overline{x}_2} \overline{\tau}_{\overline{y}=-\overline{h}}\,d\overline{x} \quad \text{and} \quad \overline{T}_{Fh+} = -\int_{-\infty}^{\overline{x}_2} \overline{\tau}_{\overline{y}=\overline{h}}\,d\overline{x}\,. \tag{2.26}$$

3. Results and discussion

In this problem, numerical calculations are made using the following values:

$$U_1 = 400\ cm/s, \quad h_0 = 4 \times 10^{-4}\ cm, \quad R = 3\ cm, \quad \overline{T_U} = 1, \quad \overline{T_L} = 1.5\,.$$

3.1. Velocity profile

Figures (2-4) display the fluid's velocity for the regions prior to, following pressure peaks, and at the point of pressure peaks, respectively. The profiles in the first two graphs resemble parabolas with vertices pointing upward and downward in the areas prior to and after the point of pressure peak. As seen in Fig. (2), the vertices under the $\bar{y}$ line indicate that there is a reverse flow at the inlet. Prasad and Subrahmanyam [11] demonstrated reverse flow. The back flow is eliminated as the fluid moves forward [7, 11-13]. However, the velocity profile, which can be seen in Fig. (4), appears to be increasing linearly at the point of maximum pressure [11].

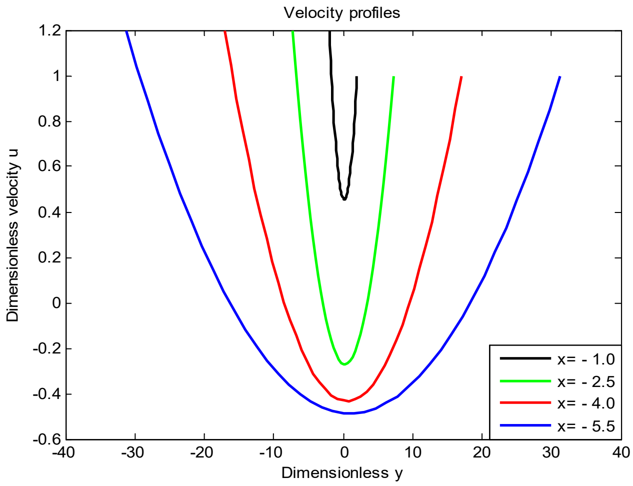

Fig.2. Velocity profile.

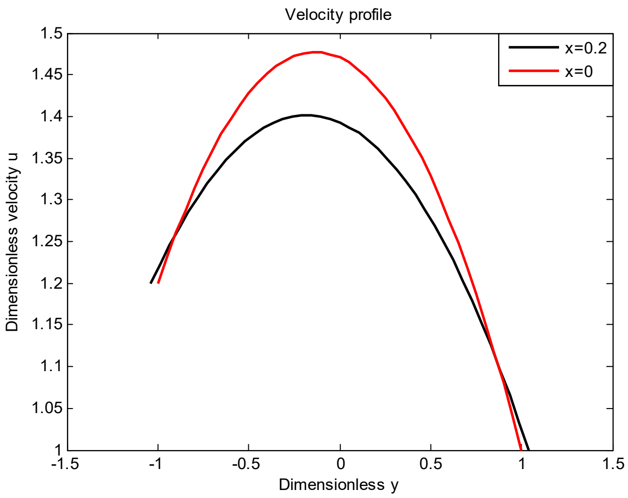

Fig.3. Velocity profile.

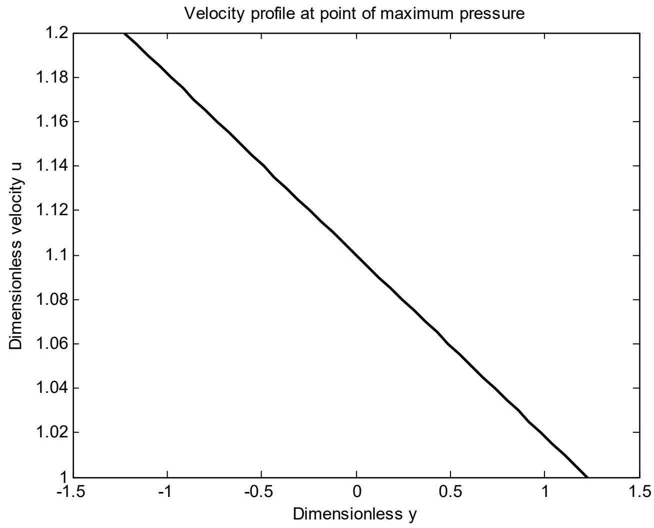

Fig.4. Velocity at pressure peak point.

3.2. Pressure profile

The dimensionless pressure $\overline{p}$ is quantitatively estimated and shown in Figs. (5-7). Figures (5) and (6) show that in the Newtonian ($\tau_0 = 0$) and non-Newtonian ($\tau_0 \neq 0$) instances, respectively, $\overline{p}$ rises as rolling ratio $\overline{U}$ rises. It shows that, in comparison to pure rolling, hydrodynamic pressure is greater in the sliding scenario. These behaviours have been described in [2, 3, 11, 14, 15]. In addition, the lubricant pressure for distinct values of τ_0 is depicted in Fig. (7) for the sliding case. It is clear from this figure that non-Newtonian fluids experience greater pressure than Newtonian fluids. The points at pressure peaks for both Newtonian and non-Newtonian fluids are also shown in Tab.1. This table shows that as the rolling ratio rises, the points of maximum pressure move toward and away from the centre line of contact, for $\tau_0 = 1$ and $\tau_0 = 0$, respectively. Revathi *et al.* [7] identify a similar kind of behaviour.

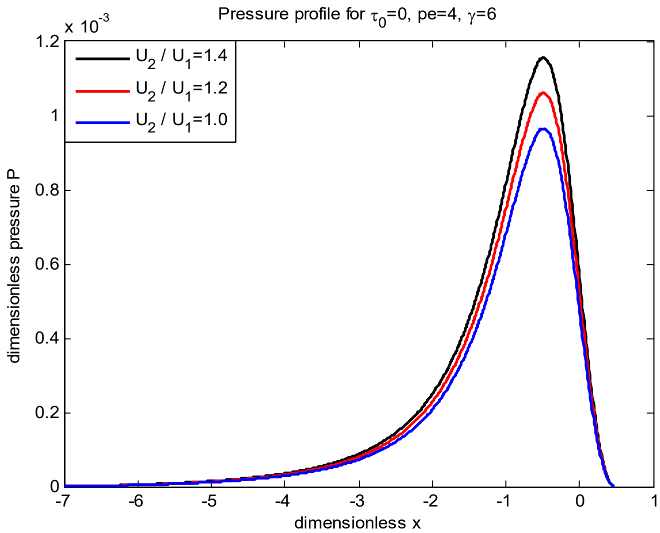

Fig.5. Pressure with respect to Ū.

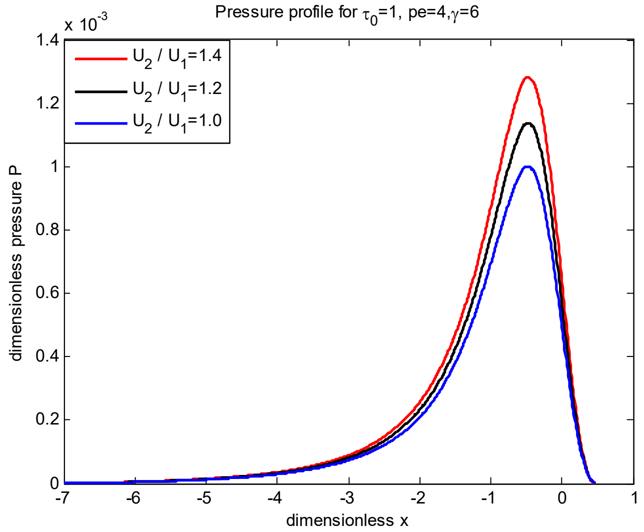

Fig.6. Pressure with respect to Ū.

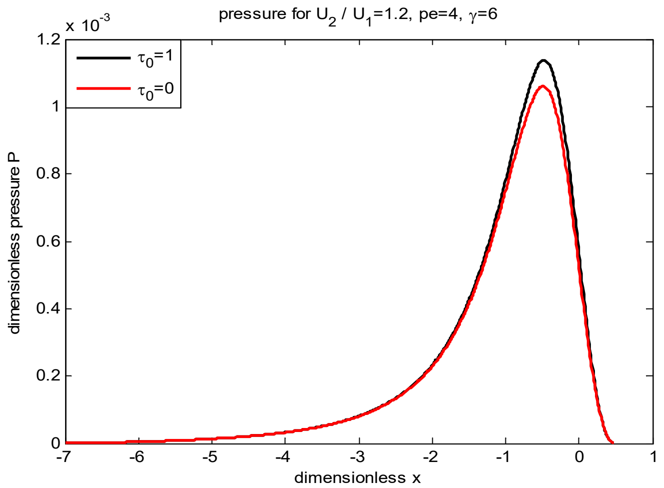

Fig.7. Pressure versus $\bar{x}$.

Table1. Points of maximum pressure.

$\bar{U}$	$\bar{\tau_0} = 0$	$\bar{\tau_0} = 1$
1.0	*0.48906795*	*0.47882541*
1.1	*0.48907111*	*0.47626241*
1.2	*0.48909541*	*0.47376241*
1.3	*0.48913241*	*0.47126241*
1.4	*0.48918241*	*0.46876241*
1.5	*0.48924437*	*0.46628241*

3.3. Viscosity ($\bar{\mu}$) profile

For distinct values of τ_0 in the sliding case, the viscosity $\bar{\mu}$ is estimated numerically and presented in Fig (8). The figure shows that the viscosity for the non-Newtonian case is greater than that of the Newtonian case.

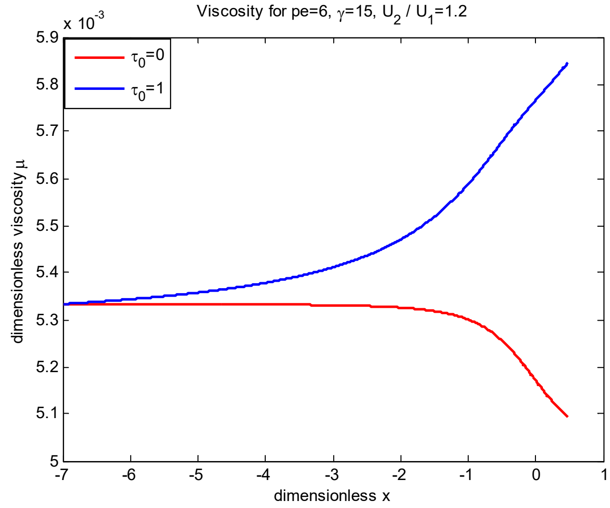

Fig.8. Effect of viscosity against $\bar{x}$.

3.4. Mean temperature profile:

Figures 9-12 show the dimensionless mean temperature $\overline{T_m}$ of the lubricant for various values of the rolling ratio $\overline{U}$ and τ_0.

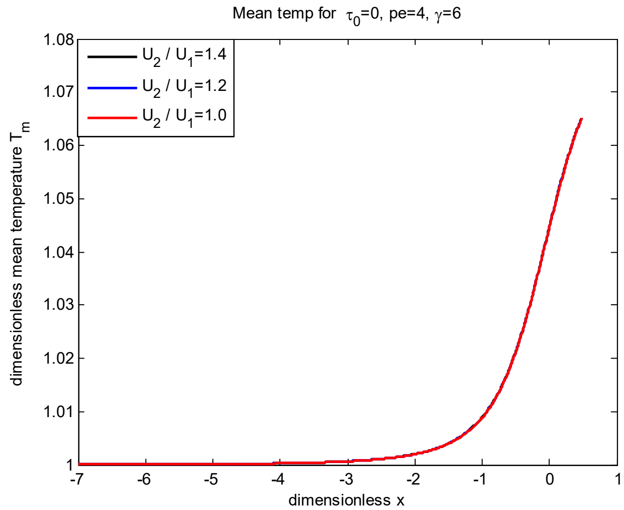

Fig.9. Effect of mean temperature against $\bar{x}$.

Figure 9, which shows the dimensionless mean temperature for distinct values of $\overline{U}$ for $\tau_0 = 0$ (Newtonian case), demonstrates that the mean temperature coincides for various values of $\overline{U}$. This shows that when a Newtonian fluid is taken into account, the effect of the rolling ratio is not substantial. Figure 10 shows the mean temperature for various values of $\overline{U}$ and for $\tau_0 = 1$ (non-Newtonian case). This graph demonstrates that the mean temperature drops as $\overline{U}$ increases. Figure 11, which displays the mean temperature for various τ_0 for sliding case ($\overline{U}$=1.2), demonstrates how the mean temperature falls as τ_0 rises. The mean temperature is shown in Fig. 12 for various values of $\overline{p_e}$ (Pecklet number) and for a constant value of $\overline{U}$=1.2. This graph demonstrates that the mean temperature rises with $\overline{p_e}$.

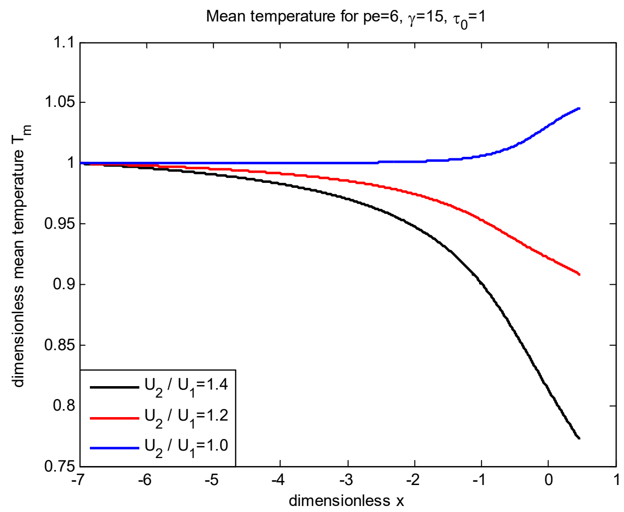

Fig.10. Effect of mean temperature against $\overline{x}$.

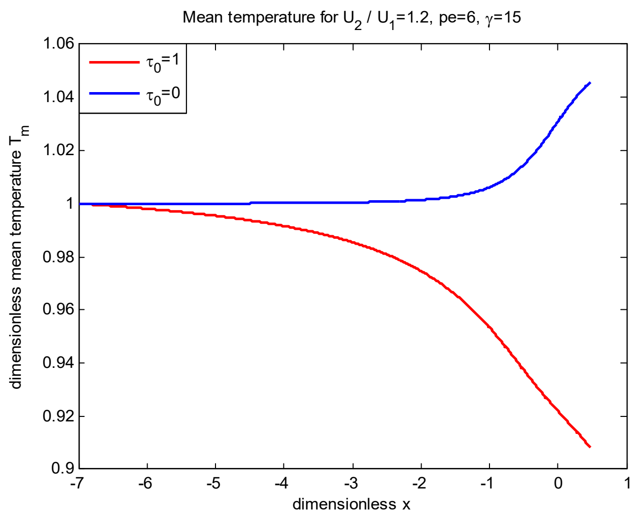

Fig.11. Effect of mean temperature against $\overline{x}$.

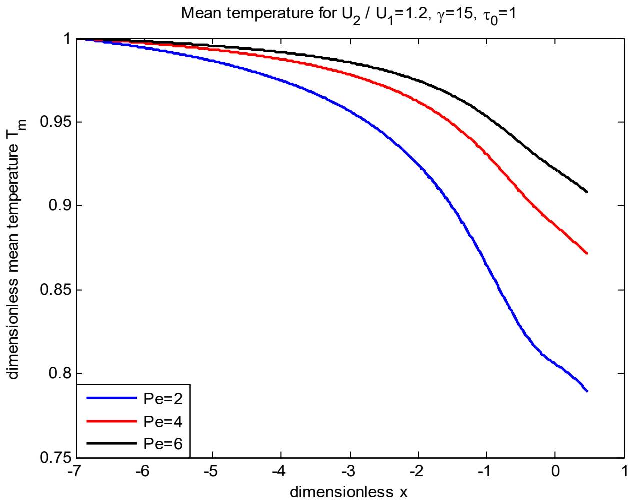

Fig.12. Effect of mean temperature against $\bar{x}$.

3.5 Load and traction

For various values of the rolling ratio $\bar{U}$ and yield stress parameter $\bar{\tau}_0$, dimensionless load values in the y-direction are calculated and shown in Tab.2. The table also demonstrates that, in both Newtonian and non-Newtonian scenarios, load rises with the rolling ratio. These findings are fairly consistent with past research findings [11-13, 15]. Further, the non-Newtonian load is larger when compared with Newtonian load for any fixed values of the rolling ratio parameter $\bar{U}$.

Table 2. Load values.

$\bar{U}$	$\overline{W_y}$ for $\bar{\tau}_0 = 0$	$\overline{W_y}$ for $\bar{\tau}_0 = 1$
1.0	*0.00150433*	*0.00154139*
1.1	*0.00157920*	*0.00163845*
1.2	*0.00165394*	*0.00173748*
1.3	*0.00172856*	*0.00183885*
1.4	*0.00180307*	*0.00194240*
1.5	*0.00187746*	*0.00204851*

Tables 3 and 4 show the computed traction forces at the lower and upper surfaces for various values of $\bar{\tau}_0$ and $\bar{U}$. Both the Newtonian and non-Newtonian cases are shown for $\bar{\tau}_0 = 0$ and $\bar{\tau}_0 = 1$ respectively here. For a certain value of $\bar{U}$, traction forces grow on the lower and higher surfaces with $\bar{\tau}_0$. Table 3 also shows that traction forces rise with $\bar{U}$, which suggests that traction forces will be higher on surfaces moving faster. These results closely resemble those found in Revathi *et al.* (2020) and Revathi *et al*. (2021). When running at the same speed, both rollers attain the same traction force.

Table 3. Traction values at lower surface.

$\overline{U}$	$\bar{\tau}_0 = 0$	$\bar{\tau}_0 = 0.5$	$\bar{\tau}_0 = 1$
1.0	0.00322508	2.79322508	5.58322508
1.1	0.00363444	2.79363444	5.58363444
1.2	0.00404381	2.79404381	5.58404381
1.3	0.00445319	2.79445319	5.58445319
1.4	0.00486258	2.79486258	5.58486258
1.5	0.00527198	2.79527198	5.58527198

Table 4. Traction values at upper surface.

$\overline{U}$	$\bar{\tau}_0 = 0$	$\bar{\tau}_0 = 0.5$	$\bar{\tau}_0 = 1$
1.0	0.00322508	2.79322508	5.58322508
1.1	0.00313841	2.79313841	5.58313841
1.2	0.00305175	2.79305175	5.58305175
1.3	0.00296509	2.79296509	5.58296509
1.4	0.00287845	2.79287845	5.58287845
1.5	0.00279181	2.79279181	5.58279181

4. Conclusion

An attempt is made to investigate the non-Newtonian incompressible Bingham plastic fluid film lubrication properties of the line contact problem for a lightly loaded rigid system. For various values of the yield stress and sliding parameters, the governing equations are solved for pressure, mean film temperature and velocity of the lubricant. The outcomes of this work can be used to support the following assertions:

- The velocity of the lubricant is independent of $\bar{\tau}_0$.
- Lubricant velocity at point of pressure peak decreases linearly.
- Pressure increases because of an increase in the rolling ratio.
- The load increases as the rolling ratio rises.
- The lower surface has greater traction than the upper surface due to its higher speed.
- Traction forces on both surfaces increase as the yield stress parameter increases.

Acknowledment

The investigators remain profusely grateful to Koneru Lakshmaiah Education Foundation, Guntur, India for extending support and assistance with required permissions during this research study at the Department of Engineering Mathematics and to Sir C.R. Reddy College of Engineering, Eluru, India for necessary permissions and extending facilities for the work.

Nomenclature

c_p – specific heat
h – film thickness
h_0 – minimum film thickness
k – thermal conductivity
p – hydrodynamic pressure
R – radius of the cylinder
TF_h – traction force
T_m – mean temperature
U_1, U_2 – velocities of the surfaces
u – fluid velocity in x-direction
v – fluid velocity in y-direction
W_y – normal load
x_1 – point of maximum pressure
x_2 – point of cavitation
β – thermal coefficient
μ – viscosity
μ_0 – viscosity coefficient
τ – shear stress
τ_0 – yield stress
ρ – density

References

[1] Dhaneshwar Prasad, Sudam Sekhar Panda and Subrahmanyam, S.V. (2012): *Non-Newtonian squeeze film lubrication of journal bearing with temperature effect.*– Int. J. of Eng. Sci. & Adv. Techn., vol.2, No.3, pp.438-444.

[2] Dhaneshwar Prasad, Subrahmanyam, S.V. and Sudam Sekhar Panda (2012): *Thermal effects in hydrodynamic lubrication of asymmetric rollers using Runge-Kutta Fehlberg method.*– Int. J. of Eng. Sci. & Adv. Techn., vol.2, No.3, pp.422-437.

[3] Venkata Subrahmanyam Sajja and Dhaneshwar Prasad (2015): *Characterization of lubrication of asymmetric rollers including thermal effects.*– Indus. Lubri. Tribol., vol.67, No.3, pp.246-255. https://doi.org/10.1108/ILT-04-2013-0048.

[4] Christopher Dorier and John Tichy, (1992): *Behavior of Bingham-like viscous fluid in lubrication flows.*– Journal of Non Newtonian Fluid Mechanics,vol.45, pp.291-310. https://doi.org/10.1016/0377-0257(92)80065-6.

[5] Milne A.A. (1954): *A theory of rheodynamic lubrication*.– Kolloidk-Z, 139 Haft 1/2, pp.96-101.

[6] Gadamsetty Revathi, Venkata Subrahmanyam Sajja and Dhaneshwar Prasad (2019): *Bingham plastic fluid film lubrication of asymmetric rollers.*– Int. J. of Sci. & Techn. Res., vol.8, No.11, pp.2549-2554.

[7] Revathi Gadamsetty, Venkata Subrahmanyam Sajja, Sudam Sekhar, P. and Dhaneshwar Prasad (2020): *Thermal effects in Bingham plastic fluid film lubrication of asymmetric rollers.*– Frontiers in Heat and Mass Transfer, vol.15, No.18, pp.1-7. http://dx.doi.org/10.5098/hmt.15.18.

[8] Dhaneshwar Prasad and Punyatma Singh (1987): *Thermal and squeezing effects in non-Newtonian fluid film lubrication of rollers*.– Wear, vol.119, pp.175-190, https://doi.org/10.1016/0043-1648(87)90107-4.

[9] Tokio Sasaki, Haruo Mori and Norio Okino, (1962): *Fluid lubrication theory of roller bearing.*– Journal of Basic Engineering, pp.166-174. https://doi.org/10.1115/1.3657241.

[10] Jang J.Y. and Khonsari M.M. (2013): *Lubrication with Newtonian fluid*.– Encyclopedia of Tribology, pp.2142-2146, Springer, Boston, MA.

[11] Dhaneshwar Prasad and Venkata Subrahmanyam Sajja (2016): *Non-Newtonian lubrication of asymmetric rollers with thermal and inertia effects*.– Trib. Trans., vol.59, No.5, pp.818-830, doi.org/10.1080/10402004.2015.1107927

[12] Prasad D., Singh P. and Sinha P. (1988): *Non-uniform temperature in non-Newtonian compressible fluid film lubrication of rollers.*– J. of Trib., vol.110, pp.653-658, https://doi.org/10.1115/1.3261708.

[13] Prasad D., Shukla J.B., Singh P., Sinha P. and Chhabra R.P. (1991): *Thermal effects in lubrication of asymmetric rollers*.– Tribol. Intl., vol.24, pp.239-246, https://doi.org/10.1016/0301-679X(91)90050-J.

[14] Gadamsetty Revathi, Venkata Subrahmanyam Sajja and Dhaneshwar Prasad (2019): *Thermal effects in power-law fluid film lubrication of rolling/sliding line contact.*– Int. J. of Innov. Technol. Explor. Eng., vol.8, No.9, pp.277-283.

[15] Dhaneshwar Prasad and Venkata Subrahmanyam Sajja (2016): *Thermal effects in non-Newtonian lubrication of asymmetric rollers under adiabatic and isothermal boundaries.*– Int. J. Chem. Sci., vol.14, No.3, pp.1641-1656.

[16] Revathi Gadamsetty, Venkata Subrahmanyam Sajja, Sudam Sekhar P. and Dhaneshwar Prasad (2021): *Squeeze film lubrication of asymmetric rollers by Bingham plastic fluid*.– Front. in Heat and Mass Trans., vol.16, No.7, pp.1-6. http://dx.doi.org/10.5098/hmt.16.7.

Received: October 8, 2022
Revised: March 7, 2023